Article

Self-Assembly of Diorganotin(IV) Oxides (R = Me, *n*Bu, Ph) and 2,5-Pyridinedicarboxylic Acid to Polymeric and Trinuclear Macrocyclic Hybrids with Porous Solid-State Structures: Influence of Substituents and Solvent on the Supramolecular Structure

Reyes Garca-Zarracino, and Herbert Hpfl

J. Am. Chem. Soc., **2005**, 127 (9), 3120-3130• DOI: 10.1021/ja0437095 • Publication Date (Web): 11 February 2005

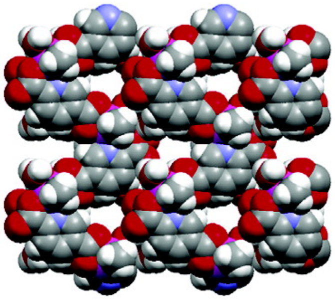

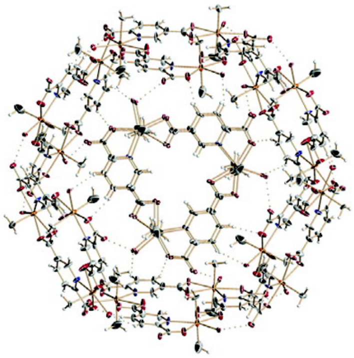

ACS Publications
High quality. High impact.

Journal of the American Chemical Society is published by the American Chemical Society. 1155 Sixteenth Street N.W., Washington, DC 20036

J|A|C|S
A R T I C L E S

Self-Assembly of Diorganotin(IV) Oxides (R = Me, *n*Bu, Ph) and 2,5-Pyridinedicarboxylic Acid to Polymeric and Trinuclear Macrocyclic Hybrids with Porous Solid-State Structures: Influence of Substituents and Solvent on the Supramolecular Structure

Reyes García-Zarracino and Herbert Höpfl*

Contribution from the Centro de Investigaciones Químicas, Universidad Autónoma del Estado de Morelos, Avenida Universidad 1001, C.P. 62210 Cuernavaca, Mexico

Received October 15, 2004; E-mail: hhopfl@buzon.uaem.mx

Abstract: 2,5-Pyridinedicarboxylic acid has been reacted with three different diorganotin(IV) oxides (R = Me, *n*Bu, Ph) to study the molecular and supramolecular structures of the resulting diorganotin(IV) 2,5-pyridinedicarboxylates. It has been found that coordinating solvent molecules can change the supramolecular structure completely. The molecular structures found are either polymeric (zigzag) or cyclotrimeric; the supramolecular arrangements include (i) systems having only loosely bound discrete molecules (van der Waals contacts), (ii) systems having a 2D or 3D hydrogen-bonded structure, and (iii) systems having a 3D polymeric coordination structure. Channels or cavities are formed in several cases. For a particular case, evidence has been provided that molecular aggregation to capsules through hydrogen bonding interactions is possible in solution.

1. Introduction

During the past few years metal-directed self-assembly has become a powerful tool for the construction of systems having cavities or possessing intrinsic physical properties that are promising for the creation of new materials.[1] More recently, metal−ligand binding has been combined with hydrogen bonding, thus allowing for the construction of an almost infinite number of new supramolecular entities.[2]

Supramolecular systems with cavities can have either discrete structures that may be explored in terms of molecular recognition and host−guest chemistry[3] or polymeric structures with voids or channels available for the inclusion of guest molecules.[4] Among them, porous materials have received special interest, since they may function as catalysts with applications similar to those known for zeolithes.[5]

Although considerable advance has been reached in the development of this branch of supramolecular chemistry, there are still some fields that have received little attention thus far by the scientific community working in this area. One of them is that in comparison to systems with transition metals and lanthanides, few supramolecular aggregates containing main group elements are known;[6,7] besides, few organometallic species have been involved in self-assembly processes.[6f,k,7a−e,i−k] Considering that (i) there is a series of organometallic compounds that have enhanced thermal and kinetic stability, including toward corrosive substances such as oxygen or water, and that (ii) organometallic reagents can carry a huge variety

---

(1) For recent reviews, see: (a) Stang, P. J. *Chem.−Eur. J.* **1998**, *4*, 19. (b) Langley, P. J.; Hulliger, J. *Chem. Soc. Rev.* **1999**, *28*, 279. (c) Hagrman, P. J.; Hagrman, D.; Zubieta, J. *Angew. Chem., Int. Ed.* **1999**, *38*, 2638. (d) Fujita, M. *Struct. Bonding* **2000**, *96*, 177. (e) Saalfrank, R. W.; Uller, E.; Demleitner, B.; Bernt, I. *Struct. Bonding* **2000**, *96*, 149. (f) Swiegers, G. F.; Malefetse, T. J. *Chem. Rev.* **2000**, *100*, 3483. (g) Holliday, B. J.; Mirkin, C. A. *Angew. Chem., Int. Ed.* **2001**, *40*, 2022. (h) Dinolfo, P. H.; Hupp, J. T. *Chem. Mater.* **2001**, *13*, 3113. (i) Feréy, G. *Chem. Mater.* **2001**, *13*, 3084. (j) Moulton, B.; Zaworotko, M. J. *Chem. Rev.* **2001**, *101*, 1629. (k) Vilar, R. *Angew. Chem., Int. Ed.* **2003**, *42*, 1460. (l) Janiak, C. *J. Chem. Soc., Dalton Trans.* **2003**, 2781. (m) Rao, C. N. R.; Natarajan, S.; Vaidhyanathan, R. *Angew. Chem., Int. Ed.* **2004**, *43*, 1466. (n) Würthner, F.; You, C.-C.; Saha-Möller, C. R. *Chem. Soc. Rev.* **2004**, *33*, 133.

(2) See, for example: (a) Burrows, A. D.; Chan, C.-W.; Chowdry, M. M.; McGrady, J. E.; Mingos, D. M. P. *Chem. Soc. Rev.* **1995**, 329. (b) Munakata, M.; Wu, L. P.; Yamamoto, M.; Kuroda-Sowa, T.; Maekawa, M. *J. Am. Chem. Soc.* **1996**, *118*, 3117. (c) Braga, D.; Grepioni, F.; Desiraju, G. R. *Chem. Rev.* **1998**, *98*, 1375. (d) Aakeröy, C. B.; Beatty, A. M.; Leinen, D. S. *Angew. Chem., Int. Ed.* **1999**, *38*, 1815. (e) Braga, D. *J. Chem. Soc., Dalton Trans.* **2000**, 3705. (f) Burrows, A. D.; Harrington, R. W.; Mahon, M. F.; Price, C. E. *J. Chem. Soc., Dalton Trans.* **2000**, 3845. (g) Beatty, A. M. *CrystEngComm* **2001**, *51*, 1. (h) Braga, D.; Maini, L.; Grepioni, F.; Elschenbroich, C.; Paganelli, F.; Schiemann, O. *Organometallics* **2001**, *20*, 1875. (i) Burrows, A. D.; Harrington, R. W.; Mahon, M. F.; Teat, S. J. *CrystEngComm* **2002**, 539. (j) Burke, N. J.; Burrows, A. D.; Donovan, A. S.; Harrington, R. W.; Mahon, M. F.; Price, C. E. *J. Chem. Soc., Dalton Trans.* **2003**, 3840. (k) Aakeröy, C. B.; Beatty, A. M.; Desper, J.; O'Shea, M.; Valdes-Martinez, J. *J. Chem. Soc., Dalton Trans.* **2003**, 3956.

(3) Apart from the reviews cited in refs 1d and 1k, see: (a) Lehn, J.-M. *Supramolecular Chemistry*; VCH: New York, 1995. (b) Philp, D.; Stoddart, J. F. *Angew. Chem., Int. Ed. Engl.* **1996**, *35*, 1154. (c) Linton, B.; Hamilton, A. D. *Chem. Rev.* **1997**, *97*, 1669.

(4) Apart from the reviews cited in refs 1b, 1c, 1f, 1i, and 1j, see: (a) Yaghi, O. M.; Li, H.; Davis, C.; Richardson, D.; Groy, T. L. *Acc. Chem. Res.* **1998**, *31*, 474. (b) Batten, S. R.; Robson R. *Angew. Chem., Int. Ed.* **1998**, *37*, 1460.

(5) See, for example: (a) Yaghi, O. M.; Li, G.; Li, H. *Nature* **1995**, *378*, 703. (b) Byrd, H.; Clearfield, A.; Poojary, D.; Reis, K. P.; Thompson, M. E. *Chem. Mater.* **1996**, *8*, 2239. (c) Li, H.; Eddaoudi, M.; O'Keeffe, M.; Yaghi, O. M. *Nature* **1999**, *402*, 276. (d) Chui, S. S.-Y.; Lo, S. M.-F.; Charmant, J. P. H.; Orpen, A. G.; Williams, I. D. *Science* **1999**, *283*, 1148. (e) Lu, J.; Mondal, A.; Moulton, B.; Zaworotko, M. J. *Angew. Chem., Int. Ed.* **2001**, *40*, 2113. (f) Kitaura, R.; Seki, K.; Akiyama, G.; Kitagawa, S. *Angew. Chem., Int. Ed.* **2003**, *42*, 428. (g) Keppert, C. J.; Prior, T. J.; Rosseinsky, M. J. *J. Am. Chem. Soc.* **2000**, *122*, 5158. (h) Prior, T. J.; Bradshaw, D.; Teat, S. J.; Rosseinsky, M. J. *Chem. Commun.* **2003**, 500. (i) Reddy, D. S.; Duncan, S.; Shimizu, G. K. H. *Angew. Chem., Int. Ed.* **2003**, *42*, 1360.

10.1021/ja0437095 CCC: $30.25

of different organic substituents, new possibilities arise for the construction of supramolecular systems, especially with respect to the fine-tuning of their chemical, physical, and structural properties.

Herein we report on the formation and characterization of a series of organometallic tin complexes, which have been derived from three different diorganotin(IV) groups, namely dimethyl-, di-*n*-butyl-, and diphenyltin, using 2,5-pyridinedicarboxylate, the anion of 2,5-pyridinedicarboxylic acid, as ligand. Although it is well-known that the combination of di-, tri-, or tetracarboxylate ligands with transition and lanthanide metal ions can lead to the formation of thermally very stable polymeric materials, which in some cases possess a microporous structure,[1m] 2,5-pyridinedicarboxylate has been used for this purpose only in very few occasions.[8]

A large number of organotin(IV) carboxylates has been prepared and structurally characterized during the last few decades, and it is known that tin centers are frequently susceptible to intermolecular C═O → Sn interactions or solvent coordination.[9] Although intermolecular C═O → Sn interactions can give rise to either polymeric or cyclooligomeric structures in the solid state that may have cavities or pores (Chart 1a),[7a−e] these interactions are too weak to withstand dissociation in solution, even in the presence of only weakly coordinating solvents.[7b,d,e,10−11] However, solution-stable cyclooligomeric diorganotin(IV) complexes with macrocyclic cavities have been recently prepared using aromatic dicarboxylates as ligands.[7k] These ligands were chosen because of two reasons: first, carboxylate groups form strong covalent bonds with diorganotin(IV) moieties and second, the spatial separation of two carboxylate groups attached to the same aromatic ring induces the formation of either a polymeric chain or a cyclooligomeric ring structure (Chart 1b).[7k]

From previous reports it is known that the reaction of diorganotin(IV) groups with 2-pyridinecarboxylate and its derivatives gives complexes with coordinative N → Sn bonds and five-membered C_2NOSn chelate rings.[11,12] From the reaction of diorganotin(IV) moieties with 2,5-pyridinedicarboxylate, complexes having a polymeric or a cyclooligomeric structure may be expected (Chart 2).

Chart 1. Organotin Carboxylates Can Have Cyclooligomeric Structures Formed through (a) C═O → Sn Intermolecular Interactions or (b) Sn−O Covalent Bonds, of Which the Latter Withstand Dissociation in Solution

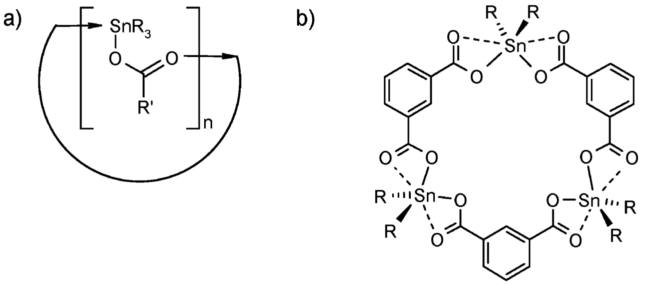

Chart 2. Reaction of Diorganotin(IV) Moieties with 2,5-Pyridinedicarboxylate Can Give Rise to Complexes Having (a) a Zigzag or Helicoidal Polymeric Structure or (b) a Cyclooligomeric Structure

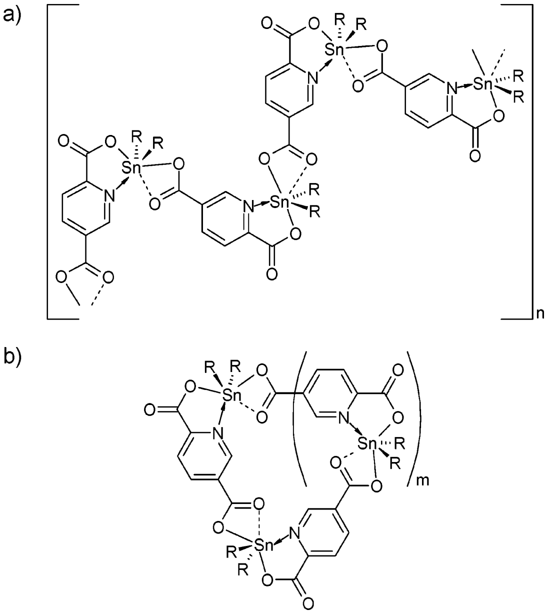

Besides the conventional analysis of the molecular and supramolecular structures as well as the host−guest chemistry of the compounds described in what follows, this report evaluates two additional parameters that are important for the design of new supramolecular systems: (i) analysis of the electronic and steric influence of the substituents attached to the metal atoms, in this case organic groups, and (ii) evaluation of the impact that solvent molecules can have on the structural characteristics of supramolecular systems, especially if they are

---

(6) For some macrocyclic or porous carboxylates containing main group elements other than tin, see: (a) Robl, C.; Weiss, A. *Z. Naturforsch. B* **1986**, *41*, 1485. (b) Robl, C.; Weiss A. *Z. Naturforsch. B* **1986**, *41*, 1490. (c) Lee, C. R.; Wang, C. C.; Wang, Y. *Acta Crystallogr., Sect. B* **1996**, *52*, 966. (d) Román, P.; Miralles, C. G.; Luque, A. *J. Chem. Soc., Dalton Trans.* **1996**, 3985. (e) Plater, M. J.; Roberts, A. J.; Marr, J.; Lachowski, E. E.; Howie, R. A. *J. Chem. Soc., Dalton Trans.* **1998**, 797. (f) Rettig, S. J.; Storr, A.; Trotter, J. *Can. J. Chem.* **1999**, *77*, 434. (g) Lightfoot, P.; Lethbridge, Z. A. D.; Morris, R. E.; Wragg, D. S.; Wright, P. A.; Kvick, A.; Vaughan, G. B. M. *J. Solid State Chem.* **1999**, *143*, 74. (h) Chen, C. Y.; Chu, P. P.; Lii, K. H. *Chem. Commun.* **1999**, 1473. (i) Kedarnath, K.; Choudhury, A.; Natarajan, S. *J. Solid State Chem.* **2000**, *150*, 324. (j) Hung, L. C.; Kao, H. M.; Lii, K. H. *Chem. Mater.* **2000**, *12*, 2411. (k) Uhl, W. *Chem. Soc. Rev.* **2000**, *29*, 259. (l) Choi, C. T. S.; Anokhina, E. V.; Day, C. S.; Zhao, Y.; Taulelle, F.; Huguenard, C.; Gan, Z.; Lachgar, A. *Chem. Mater.* **2002**, *14*, 4096. (m) Huang, Y. F.; Lii, K. H. *J. Chem. Soc., Dalton Trans.* **1998**, 4085.

(7) For macrocyclic or porous carboxylates containing tin, see: (a) Lockhart, T. P. *Organometallics* **1988**, *7*, 1438. (b) Ng, S. W.; Das, V. G. K.; Pelizzi, G.; Vitali, F. *Heteroatom Chem.* **1990**, *1*, 433. (c) Meunier-Piret, J.; Boualam, M.; Willem, R.; Gielen M. *Main Group Met. Chem.* **1993**, *16*, 329. (d) Gielen, M.; Khloufi, A. E.; Biesemans, M.; Kayser, F.; Willem, R. *Organometallics* **1994**, *13*, 2849. (e) Gajda-Schranz, K.; Nagy, L.; Kuzmann, E.; Vértes A.; Holecek, J.; Lycka, A. *J. Chem. Soc., Dalton Trans.* **1997**, 2201. (f) Natarajan, S.; Vaidhyanathan, R.; Rao, C. N. R.; Ayyappan, S.; Cheetham, A. K. *Chem. Mater.* **1999**, *11*, 1633. (g) Salami, T. O.; Zavilij, P. Y.; Oliver, S. R. J. *Acta Crystallogr.* **2001**, *E57*, m111. (h) Natarajan, S. *J. Solid State Chem.* **1998**, *139*, 200. (i) Ma, C.; Jiang, Q.; Zhang, R.; Wang, D. *J. Chem. Soc., Dalton Trans.* **2003**, 2975. (j) Ma, C.; Jiang, Q.; Zhang, R. *J. Organomet. Chem.* **2003**, *678*, 148. (k) García-Zarracino, R.; Ramos-Quiñones, J.; Höpfl, H. *Inorg. Chem.* **2003**, *42*, 3835.

(8) Shiu, K.-B.; Chen, Z.-W.; Liao, F.-L.; Wang, S.-L. *Acta Crystallogr., Sect. E* **2003**, *59*, m1072.

(9) For reviews, see: (a) Tiekink, E. R. T. *Appl. Organomet. Chem.* **1991**, *5*, 1. (b) Chandrasekhar, V.; Nagendran, S.; Baskar, V. *Coord. Chem. Rev.* **2002**, *235*, 1.

(10) Wengrovius J. H.; Garbauskas, M. F. *Organometallics* **1992**, *11*, 1334.

(11) (a) Lockhart, T. P.; Davidson, F. *Organometallics* **1987**, *6*, 2471. (b) Dakternieks, D.; Duthie, A.; Smyth, D. R.; Stapleton, C. P. D.; Tiekink, E. R. T. *Organometallics* **2003**, *22*, 4599. (c) Ma, C.; Han, Y.; Zhang, R.; Wang, D. *J. Chem. Soc., Dalton Trans.* **2004**, 1832.

(12) (a) Aizawa, S.; Natsume, T.; Hatano, K.; Funahashi, S. *Inorg. Chim. Acta* **1996**, *248*, 215. (b) Huber, F.; Preut, H.; Hoffmann, E.; Gielen, M. *Acta Crystallogr.* **1989**, *C45*, 51. (c) Gielen, M.; Joosen, E.; Mancilla, T.; Jurkschat, K.; Willem, R.; Roobol, C.; Bernheim, J.; Atassi, G.; Huber, F.; Hoffmann, E.; Preut, H.; Mahieu, B. *Main Group Met. Chem.* **1987**, *10*, 147. (d) Ng, S. W.; Raj, S. S. S.; Razak, I. A.; Fun, H.-K. *Main Group Met. Chem.* **2000**, *23*, 193.

Table 1. Crystallographic Data for Compounds **1**-H_2O, **2**-MeOH, **2**-DMSO, **2**-H_2O/EtOH, and **3**-DMSO

	1-H_2O	**1**-MeOH[a]	**2**-DMSO	**2**-H_2O/PrOH[a]	**3**-DMSO
			Crystal Data[b]		
formula	$C_9H_{11}NO_5Sn$, EtOH	$C_{45}H_{63}N_3O_{12}Sn_3$, 3 MeOH, H_2O	$C_{51}H_{81}N_3O_{15}S_3Sn_3$, 3 DMSO	$C_{45}H_{69}N_3O_{15}Sn_3$, 3 PrOH, 1.5 H_2O	$C_{63}H_{57}N_3O_{15}S_3Sn_3$, 5 DMSO
crystal size (mm^3)	0.18 × 0.24 × 0.42	0.23 × 0.11 × 0.08	0.11 × 0.11 × 0.21	0.16 × 0.16 × 0.18	0.12 × 0.20 × 0.26
MW (g mol^{-1})	377.95	1308.20	1662.82	1455.41	1939.01
space group	$P2_1/c$	Cc	$P6_3/m$	$I23$	$P\bar{1}$
			Cell Parameters		
a (Å)	11.5608(11)	26.594(4)	16.214(14)	25.1483(10)	17.878(3)
b (Å)	12.2314(12)	9.5792(14)	16.214(14)	25.1483(10)	17.958(3)
c (Å)	11.4007(11)	24.200(4)	17.23(2)	25.1483(10)	18.053(3)
α (deg)	90	90	90	90	102.151(3)
β (deg)	111.596(2)	114.730(3)	90	90	104.815(4)
γ (deg)	90	90	120	90	119.645(3)
V (Å^3)	1498.9(3)	5599.6(14)	3923(7)	15904.7(11)	4460.9(14)
Z	4	4	2	8	2
μ (mm^{-1})	1.724	1.552	1.167	0.991	1.084
ρ_{calcd} (gcm^{-3})	1.675	1.394	1.408	1.216	1.444
			Data Collection		
θ limits (deg)	$2 < \theta < 26$	$2 < \theta < 26$	$2 < \theta < 26$	$2 < \theta < 25.5$	$2 < \theta < 26$
hkl limits	−14, 14; −15, 15; −14, 14	−25, 32; −11, 11; −29, 26	−20, 20; −20, 19; −21, 21	−30, 22; −27, 30; −30, 30	−22, 22; −22, 22; −22, 22
No. collected reflns	11452	14271	40873	40446	46940
No. indep. reflns (R_{int})	2937 (0.033)	8077 (0.072)	2658 (0.099)	4960 (0.071)	17452 (0.117)
No. observed reflns[c]	2644	6879	1762	4859	7604
No. params	183	384	181	215	862
			Refinement		
R^d	0.036	0.075	0.061	0.092	0.090
$R_w{}^e$	0.082	0.151	0.201	0.228	0.291
GOF	1.172	1.086	1.098	1.280	0.963
$\Delta\rho_{min}$ (e Å^{-3})	−0.60	−2.22	−0.91	−1.19	−0.75
$\Delta\rho_{max}$ (e Å^{-3})	1.10	1.58	1.51	1.69	1.11

[a] Data collection at 100 K. [b] Data collection on a Bruker Apex CCD diffractometer, $T = 293$ K, Mo Kα, monochromator: graphite. [c] $F_o > 4\sigma(F_o)$. [d] $R = \sum(F_o{}^2 - F_c{}^2)/\sum F_o{}^2$. [e] $R_w = [\sum w(F_o{}^2 - F_c{}^2)^2/\sum w(F_o{}^2)^2]^{1/2}$.

Chart 3. Molecular Structures of Compounds **1**−**3**

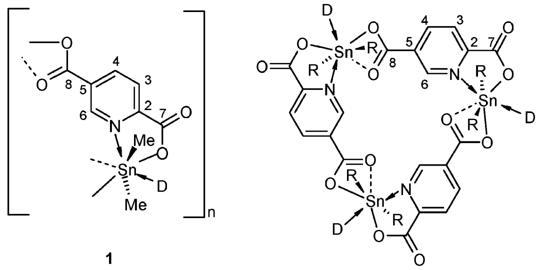

1

2 R = *n*Bu
3 R = Ph

D = solvent or C=O⟶Sn intermolecular interaction

coordinated to the metal centers. Part of the results described herein have been published in a previous communication.[13]

2. Results and Discussion

2.1. Synthetic Procedures. The equimolar reaction of dimethyltin(IV) oxide with 2,5-pyridinedicarboxylic acid in a 5:1 solvent mixture of toluene and ethanol gave, according to elemental analysis, a complex with the composition [{Me_2Sn-(2,5-pdc)}$_n$] (**1**; 2,5-pdc = 2,5-pyridinedicarboxylate) in 76% yield. Using di-*n*-butyltin and diphenyltin(IV) oxide instead of dimethyltin oxide, we obtained complexes with the composition [{R_2Sn(2,5-pdc)(H_2O)}$_3$] (**2**-H_2O; R = *n*Bu, **3**-H_2O; R = Ph) in yields of 76 and 81% (Chart 3). That these complexes are cyclotrimeric and contain solvent molecules coordinated to the tin atoms has been shown by X-ray diffraction studies, which are discussed below. All three compounds have high melting or decomposition points (>270 °C) and are stable in the air. While compound **1** is not soluble, compounds **2**-H_2O and **3**-H_2O are slightly soluble in polar solvents such as methanol, dimethyl sulfoxide, dimethoxyethane, and pyridine; these coordinating solvents can contribute to the dissociation of intermolecular interactions such as hydrogen bonds and coordinative bonds and can coordinate to the tin atoms (vide infra).

2.2. Structural Characterization in the Solid State. To obtain information on the molecular structures of compounds **1**−**3**, X-ray crystallographic studies have been performed that have shown that in all cases the solid-state coordination number of the tin atoms is seven. A total of six different crystal structures have been determined for the three compounds, showing that the heptacoordination is achieved either by the coordination of solvent molecules such as DMSO or H_2O to the tin atoms or by intermolecular C═O → Sn coordination between neighboring molecules.

Crystals of [{[Me_2Sn(2,5-pdc)(H_2O)]·EtOH}$_n$] (**1**-H_2O) could be grown by slow diffusion of a solution of potassium 2,5-pyridinedicarboxylate in ethanol into a solution of dimethyltin dichloride in a mixture of ethanol and water. The most relevant crystallographic and selected geometric data for **1**-H_2O have been summarized in Tables 1 and 2. A fragment of the polymeric molecular structure of **1**-H_2O is shown in Figure 1a.

As in all cases to be discussed in what follows, the coordination environment of the tin atoms is distorted bipyramidal-pentagonal, the axial positions being occupied by the organic substituents and the equatorial positions being shared

---

(13) García-Zarracino, R.; Höpfl, H. *Angew. Chem., Int. Ed.* **2004**, *43*, 1507.

Table 2. Selected Bond Lengths (Å) and Bond Angles (degrees) for Compounds **1**-H_2O, **2**-MeOH, **2**-DMSO, **2**-H_2O/EtOH, and **3**-DMSO

	1-H_2O	**2**-MeOH[a]	**2**-DMSO	**2**-H_2O/PrOH	**3**-DMSO[a]
		Bond Lengths			
Sn−O1	2.253(2)	2.247(9)	2.182(6)	2.222(8)	2.167(9)
Sn−O3	2.375(3)	2.335(10)	2.349(7)	2.284(8)	2.296(9)
Sn−O4	2.372(3)	2.442(9)	2.609(7)	2.475(9)	2.548(9)
Sn−O_D[b]	2.266(3)	2.261(9)	2.236(7)	2.291(8)	2.197(8)
Sn−N1	2.397(3)	2.425(11)	2.396(7)	2.373(10)	2.431(10)
Sn−C[c]	2.095(4)	2.125(13)	2.135(12)	2.138(15)	2.148(9)
		Bond Angles			
O1−Sn−O3	147.9(1)	158.0(3)	156.0(2)	153.3(3)	157.5(3)
O1−Sn−N1	70.0(1)	69.9(3)	72.3(2)	70.8(3)	70.9(3)
O1−Sn−O_D[d]	78.6(1)	81.1(3)	80.0(2)	77.4(3)	77.4(3)
O3−Sn−O4	54.9(1)	54.6(3)	52.5(3)	55.2(3)	54.4(3)
O3−Sn−O_D[d]	133.5(1)	77.6(3)	76.0(3)	76.1(3)	80.2(3)
O3−Sn−N1	77.9(1)	131.6(3)	131.7(2)	135.8(3)	131.5(3)
O4−Sn−N1	132.8(1)	77.4(3)	79.1(3)	80.8(3)	77.2(3)
O_D−Sn−N1[b]	148.4(1)	150.7(3)	152.3(3)	148.1(3)	148.1(3)
C−Sn−O1[d]	89.7(2)	89.8(5)	95.1(3)	92.6(6)	91.3(4)
C−Sn−O3[d]	90.2(2)	89.8(5)	85.6(3)	89.7(6)	89.3(4)
C−Sn−O_D[b,d]	91.9(2)	89.1(4)	91.6(3)	88.9(5)	91.3(4)
C−Sn−N1[d]	91.3(2)	90.8(5)	90.9(3)	91.5(5)	89.5(4)
C−Sn−C	178.6(2)	175.0(5)	169.7(6)	175.7(7)	176.6(4)

[a] Mean values for all three tin atoms. [b] D = donor atom from Lewis base coordinated to the tin atoms: H_2O for **1**-H_2O; C═O2 for **2**-MeOH; DMSO for **2**-DMSO, **2**-H_2O/PrOH, and **3**-DMSO. [c] Mean values for all Sn−C bonds. [d] Mean values for all analogous bond angles involving Sn−C bonds.

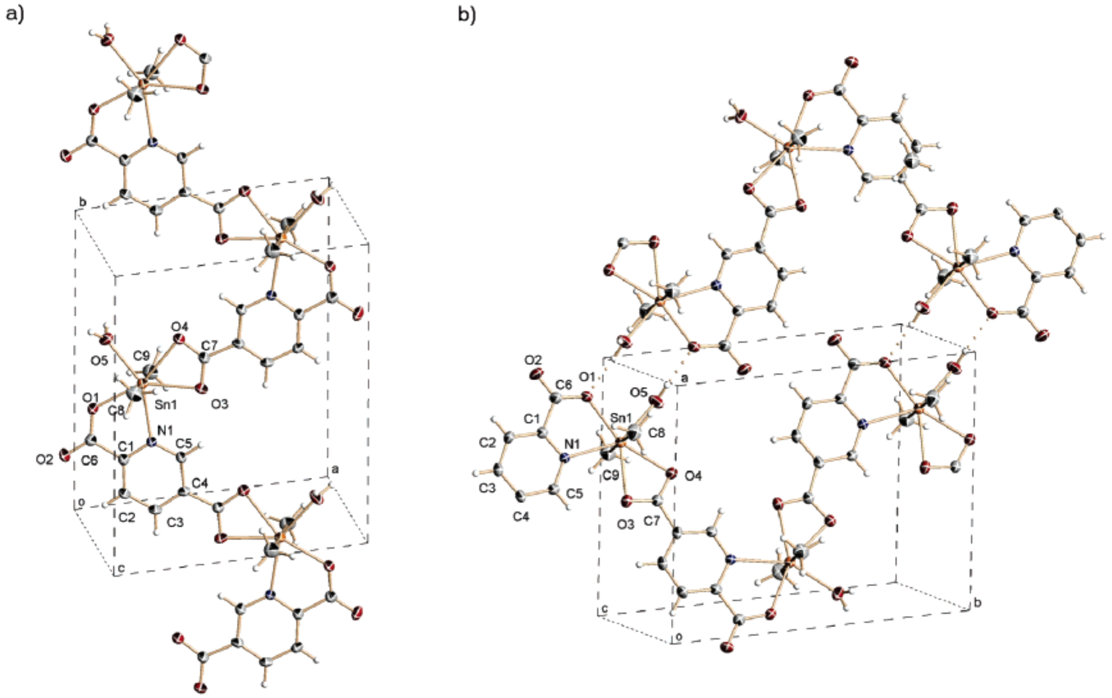

Figure 1. (a) Fragment of the polymeric structure of compound **1**-H_2O in the solid state. (b) Intermolecular hydrogen-bonding interactions in the crystal lattice of **1**-H_2O give rise to 34-membered hexanuclear macrocycles.

by the coordinating atoms of the ligand as well as an additional Lewis base, which may be a solvent molecule or an intermolecular C═O→Sn bond. Because of the chelate ring formation the carboxylate group in position 2 is monodentate, while the one in position 5 is anisobidentate, as is commonly observed for diorganotin(IV) dicarboxylates.[9]

The polymeric molecules of **1**-H_2O have a zigzag structure with 2_1 symmetry. In the crystal lattice, neighboring polymeric chains are related to each other by inversion centers, and a 2D hydrogen-bonded layer is generated. For the formation of this supramolecular structure, the tin-coordinated water molecules play a crucial role, since each of them participates in an intermolecular hydrogen bond to the oxygen atom O1 of a five-membered chelate ring (1.92 Å, 2.77 Å, 171°). This interconnection gives rise to eight-membered hydrogen-bonded rings of the composition $Sn_2O_4H_2$ and 34-membered hexanuclear supramolecular macrocycles (Figure 1b). The dimensions of the cavities of these macrocycles can be described by the schematic representation outlined in Chart 4a. They are filled with four ethanol molecules, half of which are located above and half of which are located below each 2D hydrogen bonded layer (see Supporting Information). Each ethanol molecule is involved in two hydrogen bonds, one with a tin-coordinated water molecule (1.81 Å, 2.66 Å, 171°) and the other one with the uncoordinated oxygen atom O2 of the carboxylate group in position 2 (1.94

Chart 4. Schematic Representations Showing the Dimensions of the Cavities Found in the Crystal Structures of (a) **1**-H_2O, (b) **2**-MeOH, and (c) **2**-H_2O/PrOH[a]

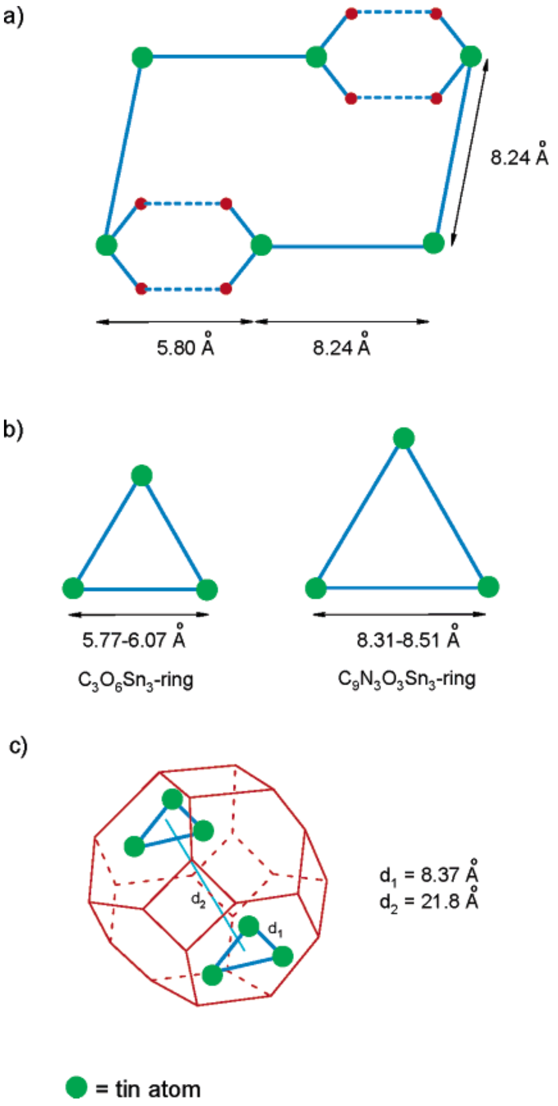

[a] In **2**-H_2O/PrOH, the trinuclear macrocycles are organized in form of a truncated octahedron (for clarity, only one pair of macrocycles has been marked).

Å, 2.74 Å, 167°). Since these hydrogen bonds are formed to donor/acceptor atoms of two different 2D layers, an overall 3D hydrogen-bonded network is resulting. If the ethanol molecules are omitted, channels crossing the whole crystal lattice are detected along axis *c* (Figure 2).

For compounds **2** and **3**, three different types of supramolecular structures have been identified. Crystals grown from a solution of **2**-H_2O in methanol gave a polymeric coordination network of the composition $[\{[(n\mathrm{Bu})_2\mathrm{Sn}(2,5\text{-pdc})]\cdot 3\mathrm{MeOH}\cdot \mathrm{H_2O}\}_n]$ (**2**-MeOH), crystals grown from solutions of **2**-H_2O and **3**-H_2O in dimethyl sulfoxide gave crystal lattices containing discrete molecules of the composition $[\{\mathrm{R_2Sn}(2,5\text{-pdc})(\mathrm{DMSO})\}_3\cdot n\mathrm{DMSO}]$ (**2**-DMSO with R = *n*Bu, *n* = 3 and **3**-DMSO with R = Ph, *n* = 5), and crystals grown from a solution of **2** in solvent mixtures of EtOH/H_2O and PrOH/H_2O gave 3D hydrogen-bonded networks of the composition $[\{[(n\mathrm{Bu})_2\mathrm{Sn}(2,5\text{-pdc})(\mathrm{H_2O})]_3\cdot 1.5\mathrm{H_2O}\cdot 3\mathrm{ROH}\}_n]$ (**2**-H_2O/EtOH with R = Et and **2**-H_2O/PrOH with R = Pr). The most relevant crystallographic and selected geometric data are outlined in Tables 1 and 2. The molecular structures for **2**-MeOH, **2**-DMSO, **3**-DMSO, and **2**-H_2O/PrOH are shown in Figures 3−6. For clarity, in Figures 3, 4, and 6 the β, γ, and δ carbon atoms of the Sn-butyl groups have been omitted. The molecular and crystal structure of **2**-H_2O/EtOH is very similar to that found for **2**-H_2O/PrOH and has been described in a previous communication.[13]

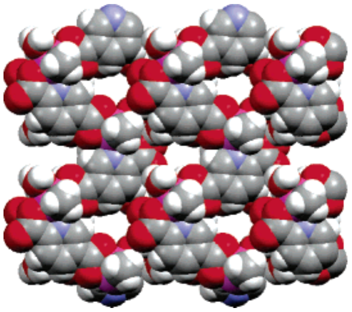

Figure 2. If the solvent guest molecules (EtOH) are omitted in the crystal structure of **1**-H_2O, channels are detected along axis *c*.

In the crystal structures of **2**-MeOH, **2**-DMSO, **3**-DMSO, and **2**-H_2O/PrOH trinuclear tin complexes are present, which are characterized by an 18-membered $C_9N_3O_3Sn_3$ macrocyclic ring containing three N→Sn coordinative bonds. It should be noticed that the overall macrocyclic structure is held together by covalent Sn−O bonds, thus providing sufficient thermodynamic stability for existence in solution (vide infra). The cavities of these macrocyclic rings are hydrophobic, consisting of three oxygen atoms and three pyridine−CH hydrogens (Chart 5). The intraannular O···O bond distances are 4.65−4.78, 4.58, 4.57−4.65, and 4.63 Å for **2**-MeOH, **2**-DMSO, **3**-DMSO, and **2**-H_2O/PrOH, respectively; the corresponding Sn···Sn distances are 8.31−8.51, 8.54, 8.50−8.57, and 8.37 Å. The hydrophobic character of this cavity is enhanced by the organic groups attached to the tin atoms, which are oriented almost perpendicular to the pentagonal NO_4 plane surrounding the tin atoms, C−Sn−C = 172.4(6)−176.6(6)° for **2**-MeOH, 169.7(6)° for **2**-DMSO, 173.2(4)−178.5(4)° for **3**-DMSO, and 175.7(7)° for **2**-H_2O/PrOH. The distances between the C−H hydrogen atoms and the neighboring oxygen atoms in the interior of the macrocyclic cavity are significantly shorter than the sum of the van der Waals radii of hydrogen and oxygen (2.70 Å), 2.39−2.63 Å for **2**-MeOH, 2.47−2.54 Å for **2**-DMSO, 2.40−2.56 Å for **3**-DMSO, and 2.47−2.52 Å for **2**-H_2O/PrOH. Thus, an interesting cyclic H_3O_3 system with a total of three bifurcated hydrogen bridges is generated (Chart 5).

According to the X-ray crystallographic data, the trinuclear molecular structures in **2**-MeOH and **3**-DMSO are asymmetric (point group C_1), while they possess crystallographic C_{3h} point group symmetry in **2**-DMSO and **2**-H_2O/PrOH. The macrocycles in **2**-DMSO and **2**-H_2O/PrOH are perfectly planar, and those in **3**-DMSO are almost planar, having OCCC torsion angles close to zero, −6.6(17) to +4(2)°. Only the macrocyclic structure of **2**-MeOH has a significant nonplanar conformation (Figure 3b), with the carboxylate-pyridine torsion angles varying from −20(2) to +13(2)°. Upon analyzing the molecular and crystal structures with respect to the conformational variation of the macrocyclic ring structures, we detected that the steric bulk of the tin-coordinated Lewis base plays a significant role. In contrast to **2**-DMSO, **3**-DMSO, and **2**-H_2O/PrOH, where solvent molecules are coordinated to the tin atoms, in **2**-MeOH

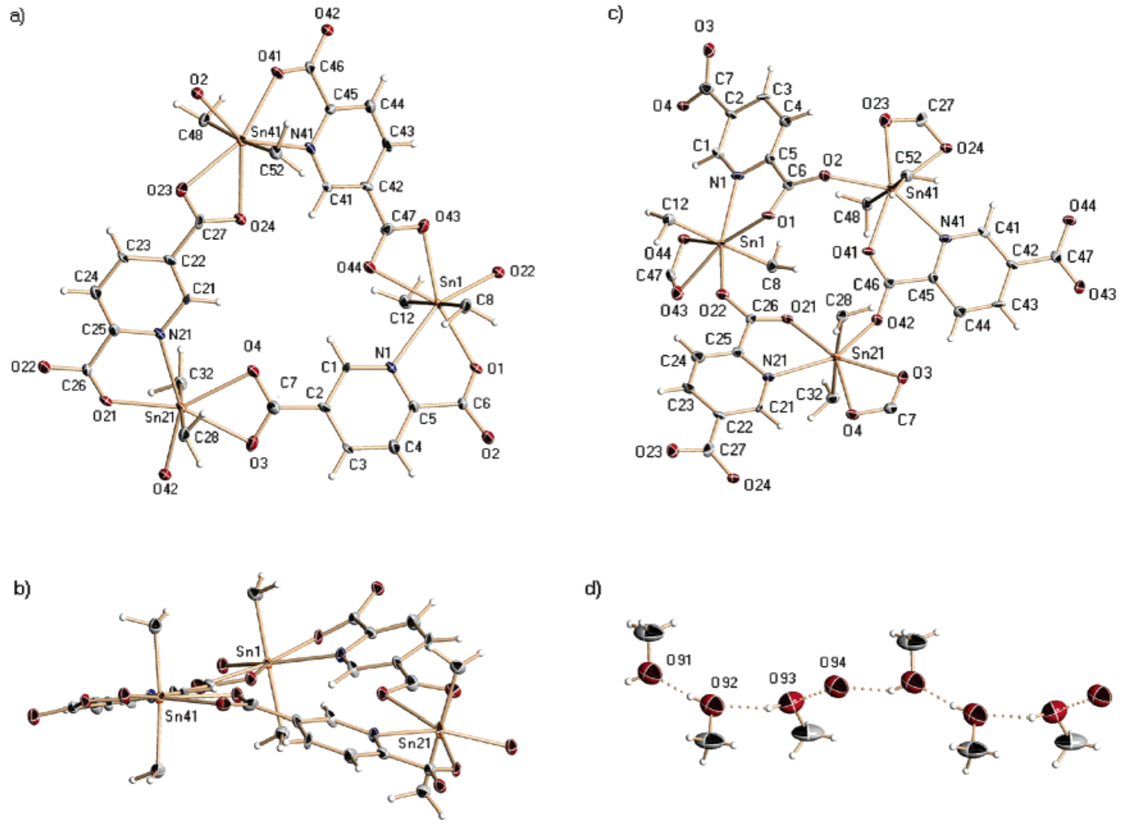

Figure 3. (a) Top and (b) lateral view of the cyclotrimer found in the crystal structure of **2**-MeOH; for clarity the somewhat disordered *β*, *γ*, and *δ* carbon atoms of the Sn-butyl groups have been omitted. (c) Twelve-membered $C_3O_6Sn_3$ heterocyclic rings formed through C═O → Sn interactions in **2**-MeOH. (d) Hydrogen-bonded helices containing methanol and water molecules in a proportion of 3:1 are found in the channels of **2**-MeOH.

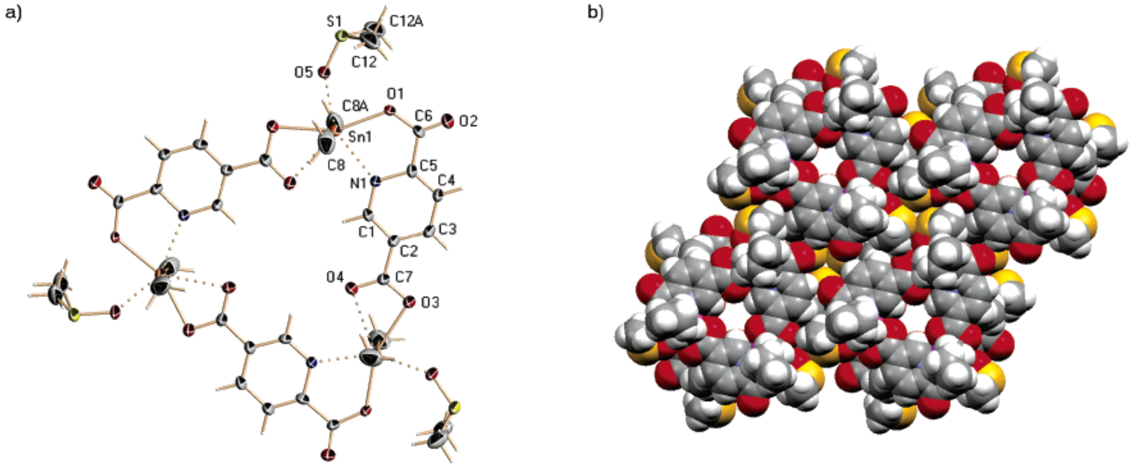

Figure 4. (a) Molecular structure of compound **2**-DMSO; for clarity the somewhat disordered *β*, *γ*, and *δ* carbon atoms of the Sn-butyl groups have been omitted. (b) Space-filling model of the crystal lattice showing the channels found for **2**-DMSO.

intermolecular C═O→Sn interactions are occurring between neighboring macrocycles, Sn−O = 2.213(9)−2.329(9) Å. Because of the conformational distortion caused by this coordination (Figure 3b), a 3D coordination polymer has been formed.

Besides the already described $C_9N_3O_3Sn_3$ macrocycles, one further type of heterocyclic ring is present in the crystal lattice of **2**-MeOH (Figure 3c). Each of these 12-membered $C_3O_6Sn_3$ heterocycles is surrounded by three 18-membered $C_9O_3N_3Sn_3$ macrocycles and vice versa. The cavities of the two heterocycles have diameters of 0.5 and 2.3 Å and are schematically described in Chart 4b. The crystal lattice of this 3D polymer possesses channels corresponding to 19.5% of the total volume,[14] in which hydrogen-bonded helices of uncoordinated solvent molecules are located. Interestingly, these helices contain simultaneously methanol and water molecules in a proportion of 3:1 (Figure 3d). Such mixed hydrogen-bonded systems are almost unknown thus far and are interesting from a biochemical point of view.[15]

In **2**-DMSO (Figure 4), **3**-DMSO (Figure 5), and **2**-H_2O/PrOH (Figure 6), solvent molecules (DMSO and H_2O) are strongly coordinated to the tin atoms, Sn−O = 2.236(7) Å for **2**-DMSO,

---

(14) *PLATON*, version 210103. Spek, A. L. *Acta Crystallogr.* **1990**, *A46*, C-34.

(15) Cheruzel, L. E.; Pometun, M. S.; Cecil, M. R.; Mashuta, M. S.; Wittebort, R. J.; Buchanan, R. M. *Angew. Chem., Int. Ed.* **2003**, *42*, 5452.

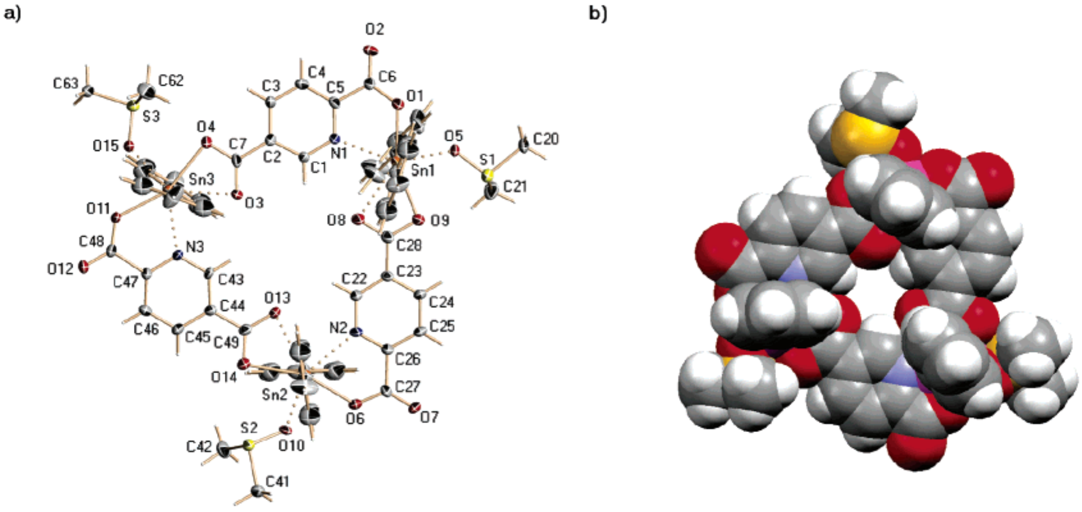

Figure 5. Molecular structure of compound **3**-DMSO. (a) ORTEP type presentation. (b) Space-filling model.

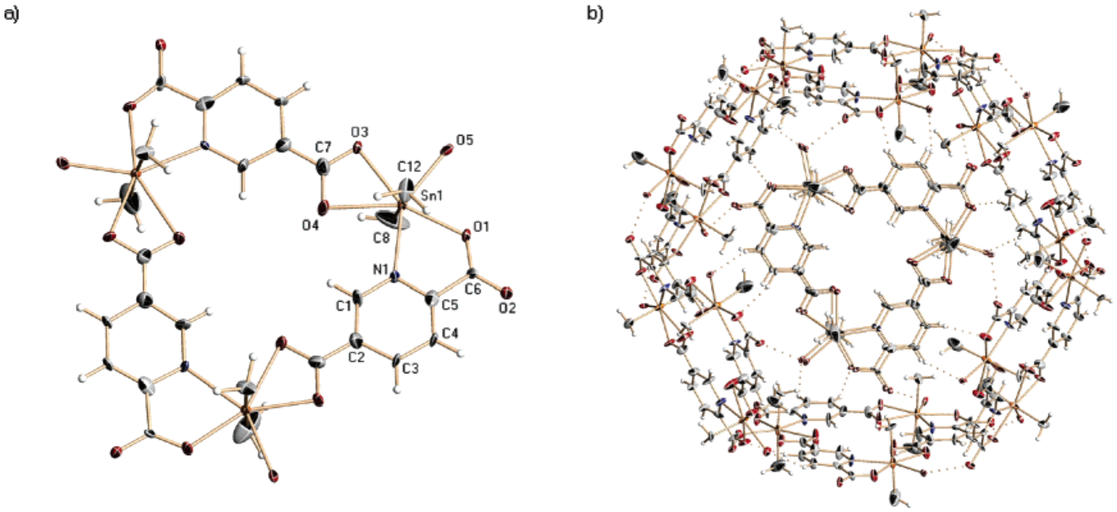

Figure 6. (a) Molecular structure of compound **2**-H_2O/PrOH; for clarity the somewhat disordered β, γ, and δ carbon atoms of the Sn-butyl groups have been omitted. (b) The unit cell of **2**-H_2O/PrOH viewed along the [111] direction showing one of the capsules present in the crystal lattice; *n*Bu groups and uncoordinated solvent molecules have been omitted for clarity.

Chart 5. Schematic Representation of the Cyclic Hydrogen-Bonding System Present in the Macrocyclic Cavities of **2**-MeOH, **2**-DMSO, **3**-DMSO, and **2**H_2O/PrOH

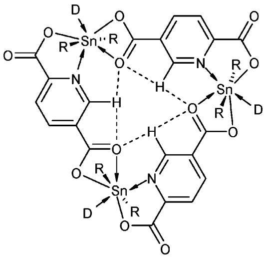

2.190(9)−2.207(7) Å for **3**-DMSO, and 2.291(8) Å for **2**-H_2O/PrOH. Interestingly, the coordinative O→Sn bonds formed with the solvent molecules are equal in length or shorter than the covalent Sn−O bonds formed with the carboxylate groups in position 5, 2.349(7) ↔ 2.236(7) Å for **2**-DMSO, 2.283(8)−2.305(9) ↔ 2.190(9)−2.207(7) Å for **3**-DMSO and 2.284(8) ↔ 2.291(8) Å for **2**-H_2O/PrOH. The only intermolecular interactions found in the crystal lattices of **2**-DMSO and **3**-DMSO are van der Waals contacts. In the case of **2**-DMSO, the macrocyclic rings are organized in a hexagonal packing mode along axis *c*, so that porous channels are formed throughout the crystal lattice (Figure 4b). The diameter of the channels is determined by the diameter of the cyclotrimeric molecules; however, there are larger voids (180 Å^3) in the space between them,[14] which are occupied by solvent molecules. Such cavities exist also in **3**-DMSO.

As for **2**-H_2O/EtOH,[13] the crystal lattice of **2**-H_2O/PrOH consists of a chiral, highly symmetrical 3D hybrid network containing trinuclear complex molecules (Figure 6a), in which each tin atom is strongly coordinated by one water molecule, Sn−O = 2.291(8) Å. The macrocycles are arranged such that large spherical cavities are formed (Figure 6b) whose centers are located at the 0,0,0 and $^1/_2$, $^1/_2$, $^1/_2$ positions in the cubic unit cell (space group *I*23). These capsules are formed through C−H···O and O−H···O hydrogen-bonding interactions between eight of the cyclotrimeric molecules and have diameters of nanodimensions (~3.5 nm).[16] Each capsule consists of 24 *n*Bu_2-Sn units and 24 ligand molecules, giving a total of 48 starting components, which are held together by covalent coordination bonds to form eight cyclotrimeric units of the composition $[\{(nBu)_2Sn(2,5\text{-pdc})(H_2O)\}_3]$ and a total of 36 hydrogen bonds

Table 3. Selected Chemical ^{1}H (400 MHz) and ^{119}Sn (149 MHz) NMR Chemical Shifts of 2,5-Pyridindedicarboxylic Acid, [{*n*Bu$_2$Sn(2,5-pdc)(solv)}$_3$] (**2**) and [{Ph$_2$Sn(2,5-pdc)(solv)}$_3$] (**3**)

	H3	H4	H6	Hα/H-o	Hβ/H-m	Hγ/H-p	Hδ	^{119}Sn–NMR
				Ligand				
DMSO-d_6	8.13 (dd)	8.41 (dd)	9.14 (dd)	–	–	–	–	–
				Compound **2**				
DMSO-d_6	8.38 (d)	8.81 (dd)	9.71 (dd)	1.31 (m)	1.28 (m)	1.08 (m)	0.62 (t)	−444
methanol-d_4	8.53 (d)	9.01 (dd)	9.83 (d)	1.52 (m)	1.27 (m)	1.17 (m)	0.68 (t)	−412
pyridine-d_5	8.87 (d)	9.16 (d)	10.80 (s)	1.84 (m)	1.42 (m)	1.04 (m)	0.53 (t)	−426
				Compound **3**				
DMSO-d_6	8.45 (d)	8.92 (dd)	9.72 (s)	7.40 (m)	7.17 (m)	7.17 (m)	–	−554

to form the sphere. The eight trinuclear molecules of each capsule occupy the hexagonal faces of a truncated octahedron, in which the centers of two opposite faces are separated by a distance of 21.8 Å (Chart 4c). In comparison to **2**-H$_2$O/EtOH, a volume increase of 1.3% is observed, indicating that the hydrogen-bonding network allows for some expansion in the presence of more voluminous alcohol molecules.

It should be noticed that these spherical supramolecular arrangements are not isolated capsules, unlike for fullerenes, but share faces with eight neighboring aggregates. Thus, the overall crystal structure can be described as a 3D network built up from the 3D union of truncated octahedra sharing all of their eight hexagonal faces with neighboring polyhedra. Each trinuclear complex (= each hexagonal face of the truncated octahedron) is involved in a total of 24 hydrogen bonds, of which 18 are required for the formation of the 3D network and six are used for connections to three propanol and three water molecules (O···O = 2.71−2.81 Å, C−H···O = 2.56−2.72 Å), which strengthen the union between the capsules in the 3D hybrid structure.

Because of the 3D arrangement described above, half of the 48 butyl groups of one capsule are oriented into its interior, while the other half contributes to the filling of another eight neighboring capsules. Although in each capsule 24 butyl groups are oriented into the interior of the cavity, large voids that have a volume of 1940 Å^3 [14] still remain in the center; cavities with such a large volume are very rare.[17] This space is filled most probably by disordered water molecules, since only smears of electron density could be detected. It should be mentioned that this is the only type of void present in the crystal structure and that their combined volumes form 24% of the crystal lattice volume. For **2**-H$_2$O/EtOH, it has been shown that this void can be occupied by hydrophobic guest molecules such as diphenylmethane (2.5 molecules in average), triphenylmethane (1.5 molecules), triptycene (3 molecules), and sodium tetraphenylborate (1 molecule).[13]

2.3. Structural Characterization in Solution. Since compounds **2**-H$_2$O and **3**-H$_2$O were slightly soluble (**3**-H$_2$O only in DMSO), NMR spectroscopic and mass spectrometric analyses could be carried out to obtain some information on their solution-state structures. The existence of the cyclotrimeric molecules could be shown by FAB$^+$ mass spectrometric studies. In both cases, it could be evidenced that the tin-coordinated water molecules can dissociate in solution, since no peaks for solvent-coordinated species were detected. For **2**, peaks corresponding to the molecular ion of a trinuclear complex and the ion formed through loss of a *n*Bu group have been detected at m/z = 1194.22 and m/z = 1136.15, respectively. For **3**, the analogous peaks appear at m/z = 1314.02 and m/z = 1235.96. Interestingly, in the mass spectrum of **2**, but not in the one of **3**, there are also peaks of minor intensity for a tetranuclear and pentanuclear species, however, with a much smaller intensity than for the trinuclear complex. The most probable explanation is that fragments of the initially trinuclear complex have recombined to higher nuclear species having the zigzag structure outlined in Chart 2 and found in the solid state for **1**-H$_2$O.

Previous ^{1}H and ^{119}Sn NMR studies on diorganotin dipicolinates have shown that N→Sn coordinative bonds that are involved in five-membered quelate rings resist dissociation in solution.[11] With respect to the coordination of Lewis bases to the tin atoms in this type of complexes, it is known that coordinating solvent molecules interact with the tin atoms in rapid exchange equilibria.[11] As expected, this is also the case for compounds **2** and **3** as shown by their ^{1}H, ^{13}C, and ^{119}Sn NMR spectra. Since these spectra have been recorded in a coordinating solvent (DMSO-d_6) it can be expected that the water molecules, which are coordinated to the tin atoms in the initially prepared complexes (vide supra), are displaced by DMSO molecules.

In the ^{1}H NMR spectra, all three signals of the central, disubstituted pyridine rings are shifted to lower fields in comparison to the ligand: $\Delta\delta$ = 0.25/0.32 ppm for H3, $\Delta\delta$ = 0.40/0.51 ppm for H4, and $\Delta\delta$ = 0.57/0.58 ppm for H6, whereby it should be noticed that the chemical shift is largest for the hydrogen atom in the α-position to the pyridine nitrogen H6 (Table 3). In the ^{13}C NMR spectra recorded in pyridine-d_5 for **2** and DMSO-d_6 for **3**, the signal of the C4 carbon atom in para orientation to the nitrogen atom is significantly downfield shifted: $\Delta\delta$ = 4.6 ppm for **2** and $\Delta\delta$ = 4.0 ppm for **3** (Table 4). Both data give evidence for the existence of the N→Sn bond.

The coordination numbers of the tin atoms in compounds **2** and **3** can be derived from their ^{119}Sn NMR spectra.[18] According to the spectra measured in DMSO-d_6, the coordination number is seven in both cases, $\delta = -444$ ppm for **2**, and $\delta = -554$ ppm for **3** (Table 3),[19] thus proving (i) the existence of the N→Sn bond and the presence of the C$_2$NOSn chelate ring, (ii) an anisobidentate coordination mode of the carboxylate group in position 5 of the pyridine ring, and (iii) the coordination of one solvent molecule to each tin atom. In any other case the

---

(16) For details, see ref 13 and Supporting Information.

(17) For reviews, see: (a) MacGillivray, L. R.; Atwood, J. L. *Angew. Chem. Int. Ed.* **1999**, *38*, 1018. (b) Hof, F.; Craig, S. L.; Nuckolls, C.; Rebek, J., Jr. *Angew. Chem., Int. Ed.* **2002**, *41*, 1489.

(18) Wrackmeyer, B. *Annu. Rep. NMR Spectrosc.* **1985**, *16*, 73.

(19) The shift differences observed for the di-*n*-butyltin and diphenyltin species are due to the different electronic properties of the substituents, and similar differences have been observed for other diorganotin(IV) complexes. The chemical shift displacements between *n*Bu$_2$SnCl$_2$ (δ = 122 ppm) and Ph$_2$SnCl$_2$ (δ = −32 ppm) can be taken as reference to evaluate the influence of the *n*-butyl and phenyl groups on the ^{119}Sn NMR shift displacements: Smith, P. J.; Tupciauskas, A. P. *Annu. Rep. NMR Spectrosc.* **1978**, *8*, 291.

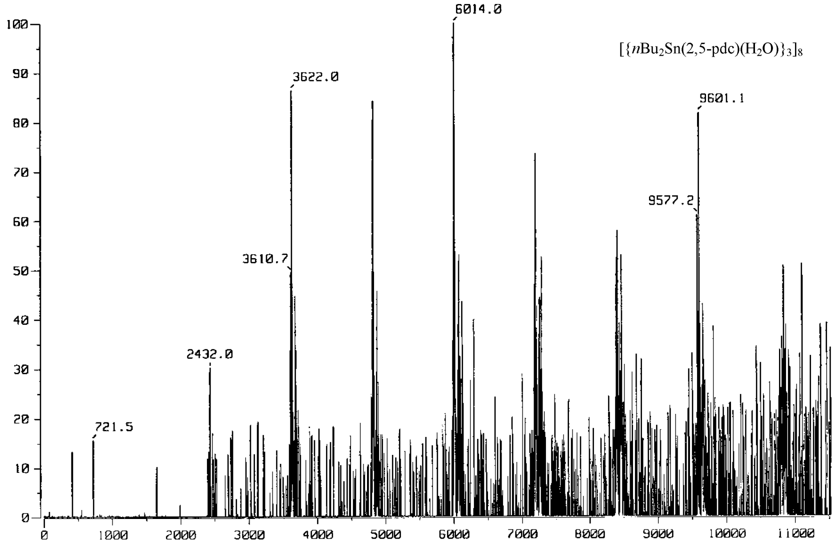

Figure 7. Cold electrospray mass spectrum showing the existence of the hydrogen-bonded capsule $[\{nBu_2Sn(2,5\text{-pdc})(H_2O)\}_3]_8$ in solution (CH_2Cl_2–MeOH, 2:1).

Table 4. Selected Chemical ^{13}C (100 MHz, DMSO-d_6) NMR Chemical Shifts of 2,5-Pyridindedicarboxylic Acid, $[nBu_2Sn(2,5\text{-}C_6H_4(COO)_2)]_3$ (**2**) and $[Ph_2Sn(2,5\text{-}C_6H_4(COO)_2)]_3$ (**3**)

	ligand	complex **2**[a]	complex **3**
C-2	151.4	152.6	150.8
C-3	124.4	126.0	125.3
C-4	138.3	143.6	143.3
C-5	129.0	133.6	131.2
C-6	149.9	149.3	147.3
C-7	165.5	166.2	163.9
C-8	165.5	172.9	171.7
C-α/C-i	–	34.4	150.1
C-*β*/C-o	–	28.2	133.1
C-*γ*/C-m	–	26.6	128.2
C-*δ*/C-p	–	13.8	128.4

[a] Data in pyridine-d_5.

coordination number would be less than seven. For the related monomeric $[Me_2Sn(picolinate)_2]$ complex, a ^{119}Sn NMR chemical shift of $\delta = -451$ ppm has been reported (in DMSO-d_6) and solvent coordination to the tin atoms has been proved.[11a] The signals in the ^{119}Sn NMR spectra of **2** and **3** are broad, confirming that the solvent molecules interact with the tin atoms in rapid exchange equilibria. The difference in the coordination mode of the two carboxylate groups present in the ligand (anisobidentate versus monodentate coordination mode) is confirmed by the fact that the ^{13}C NMR shifts of the corresponding signals are quite different from each other. While in comparison to the ligand there is only a slight shift difference for the carboxylate moieties in position 2, $\Delta\delta = 0.7$ ppm for **2** and $\Delta\delta = -1.6$ ppm for **3**, the shifts are more significant for the carboxylate groups in position 5, $\Delta\delta = 7.4$ ppm for **2** and $\Delta\delta = 6.2$ ppm for **3**, indicating a stronger anisobidentate interaction with the diorganotin(IV) group.

For the more soluble complex **2**-H_2O, the ^1H and ^{119}Sn NMR spectra have been also measured in pyridine-d_5 and methanol-d_4 to determine solvent-induced changes. Both pyridine and methanol are also coordinating solvents so that a concentration-induced substitution of the water molecules by these solvent molecules can be expected. As can be seen from Table 3, the magnetic shielding in the ^1H NMR spectrum is decreased significantly in the presence of pyridine, especially for hydrogen H6. In methanol-d_4 ($\delta = -412$ ppm) and pyridine-d_5 ($\delta = -426$ ppm), the signals in the ^{119}Sn NMR spectra of **2** are low-field shifted when compared to the spectra recorded in DMSO-d_6 ($\delta = -444$ ppm), thus indicating a somewhat weaker coordination of these solvents to the tin atoms.

Interestingly, when the ^1H NMR spectrum of compound **2**-H_2O was recorded in $CDCl_3$, two signals with a proportion of 1:1 were observed instead of one for each hydrogen atom of the pyridine ring and each methylene/methyl group of the diorganotin moieties. At first sight one might suppose that the interchange of the tin-coordinated water molecules is slower in this less polar solvent, thus giving signals for $[\{nBu_2Sn(2,5\text{-pdc})\}_3]$ and $[\{nBu_2Sn(2,5\text{-pdc})(H_2O)\}_3]$; however, a closer analysis of the structures determined by X-ray crystallography reveals that the presence or absence of tin-coordinated water molecules would hardly affect the methyl groups of the nBu_2-Sn moieties. The formation of intermolecular $C{=}O{\rightarrow}Sn$ interactions can also be excluded on the basis of previous reports on diorganotin dipicolinates, which have shown that these bonds are too weak to withstand dissociation in solution, even in unpolar solvents such as chloroform.[11]

The X-ray crystallographic studies have shown that eight cyclotrimeric molecules with the composition $[\{nBu_2Sn(2,5\text{-pdc})(H_2O)\}_3]$ can associate to capsules through hydrogen-bonding interactions (Figure 6b). One could expect that the hydrogen-bonding interactions found in these aggregates do not withstand dissociation in solution; however, in this case each trimeric molecule participates in nine hydrogen bonds at a time, so that a significant cooperative factor can be expected. A mass spectrometric study using the cold electrospray technique proved the existence of $[\{nBu_2Sn(2,5\text{-pdc})(H_2O)\}_3]_8$ in solution. From the mass spectrum shown in Figure 7, it can be seen that in solution species are present that have molecular weights corresponding to aggregates resulting form a step-by-step association/dissociation of the capsule. Therefore, it is important to note that the peak corresponding to the entire capsule has a local maximum intensity.

The existence of the capsule structure can be corroborated further by the following arguments concerning the ^1H NMR data: (i) Two different signals are observed for each hydrogen

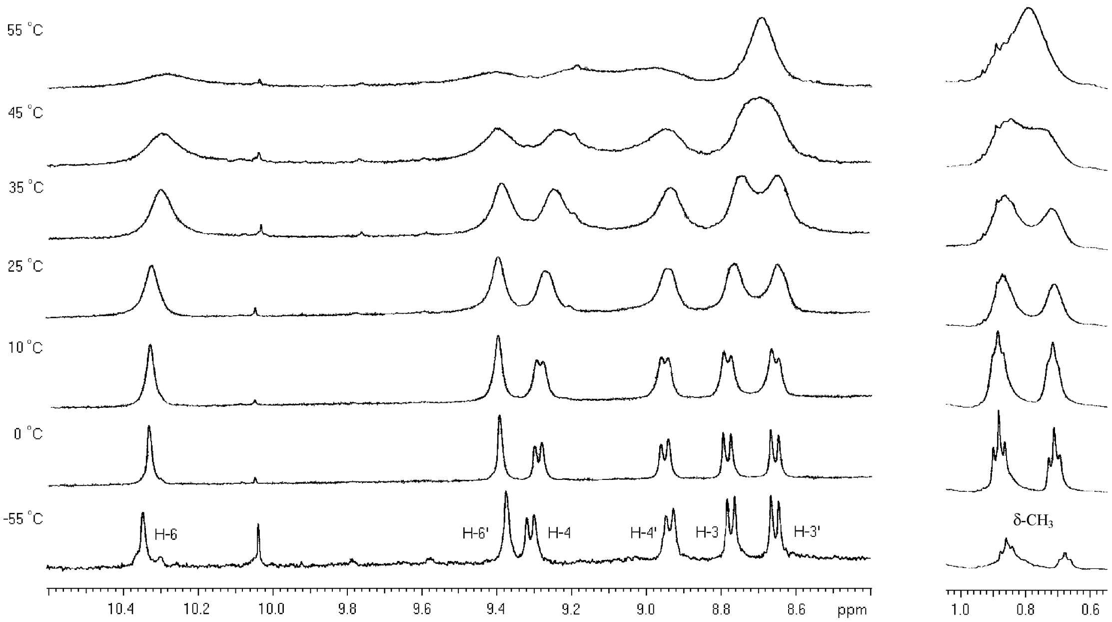

Figure 8. Variable temperature ^{1}H NMR experiment of the hydrogen-bonded capsule $[\{n\text{Bu}_2\text{Sn}(2,5\text{-pdc})(\text{H}_2\text{O})\}_3]_8$ in solution ($CDCl_3$).

atom of the pyridine ring, since the cyclotrimeric molecules participate alternately in two different hydrogen patterns; half of the molecules act as 6-fold C−H···O and 3-fold O−H···O donors, and the second half act as 6-fold C−H···O and 3-fold O−H···O acceptors (Figure 6b). (ii) The *n*-butyl groups attached to the tin atoms are in two different coordination environments; half is directed to the interior of the capsule and the other half is directed to the exterior, which explains the observation of signals with different chemical shifts for the *n*-butyl hydrogen atoms, especially for the methyl groups ($\Delta\delta \approx 0.2$ ppm). A variable temperature ^{1}H NMR experiment showed furthermore that there is a dynamic equilibrium occurring in solution (Figure 8), indicating a continuous exchange of cyclotrimeric molecules (coalescence of the signals for the methyl groups) and probably also a fluctuation of the whole hydrogen-bonding system (coalescence of the signals of the pyridine hydrogens).

3. Conclusions

In conclusion, this contribution has shown that the reaction of 2,5-pyridinedicarboxylate with dimethyl-, di-*n*-butyl, and diphenyltin moieties gives either polymeric (R = Me) or discrete cyclotrimeric structures (R = *n*Bu, Ph). The tin atoms in these complexes are Lewis acid and can form additional bonds to coordinating solvent molecules such as water, dimethyl sulfoxide, and pyridine; alternatively, they are involved in C=O→Sn intermolecular interactions.

It could be shown that both the volume of the organic substituents attached to the tin atoms and the type of solvent coordinated to them have an influence on the molecular structure and the supramolecular arrangement of the complexes. Therefore, the molecular structure can either be polymeric (zigzag) or cyclotrimeric, and the supramolecular arrangements observed include (i) systems having only loosely bound discrete molecules (van der Waals contacts), (ii) systems having a 2D or 3D hydrogen-bonded structure, and (iii) systems having a 3D polymeric coordination structure. If tin-coordinated water molecules are present, intermolecular hydrogen bonds are formed, which, because of the size of the complexes, give rise to arrangements with cavities large enough for the inclusion of guest molecules, whereby the size can be varied significantly.

^{1}H NMR and cold electrospray mass spectrometric studies proved that spherical aggregates formed through hydrogen-bonding interactions can exist in unpolar solvents, but are involved in dynamic processes.

In the case of the supramolecular structure with spherical cavities, it should be possible to modulate the diameter of the voids, varying the size of the organic substituents in the diorganotin groups. These compounds could then be further exploited for the selective trapping of labile reactive species and for conducting chemical reactions by using the cavities as reaction vessels.

4. Experimental Section

Instrumental. NMR studies were carried out with a Varian Inova 400 instrument. Standards were TMS (internal, ^{1}H, ^{13}C) and $SnMe_4$ (external, ^{119}Sn). Chemical shifts are stated in parts per million; they are positive when the signal is shifted to higher frequencies than the standard. COSY and HETCOR experiments have been carried out to assign the ^{1}H and ^{13}C spectra completely. IR spectra have been recorded on a Bruker Vector 22 FT spectrophotometer. The FAB mass spectra of **2** and **3** were obtained on a Kratos Concept IH equipment. Cold electrospray mass spectrometric measurements were realized on a JEOL JMS 700 equipment cooling the supply tube with dry ice.

Preparative Part. Poly[dimethyl-μ_2-(2,5-pyridinedicarboxylato-O,O′,N)tin] (1). A solution of 2,5-pyridinedicarboxylic acid (0.152 g, 0.910 mmol) and dimethyltin(IV) oxide (0.15 g, 0.910 mmol) in toluene/ethanol (5:1) was refluxed for 8 h using a Dean−Stark trap. After cooling to room temperature, the solvent mixture was removed under vacuum, giving **1** as a light yellow product that was washed with hot ethanol. Yield: 76%. mp 270 °C (dec). Crystals of $[\{[\text{Me}_2\text{Sn}(2,5\text{-pdc})(\text{H}_2\text{O})]\cdot\text{EtOH}\}_n]$ (**1**-H_2O) were obtained upon slow diffusion of a dimethyltin(IV) dichloride solution in EtOH into a solution of potassium 2,5-pyridinedicarboxylate in EtOH/H_2O.

Spectroscopic Data for 1: IR (KBr): $\tilde{\nu}_{\max}$: 3120 (w), 3065 (w), 2984 (w), 2922 (w), 1722 (m), 1686 (s), 1625 (s), 1575 (m), 1484 (w), 1403 (m), 1327 (m), 1291 (m), 1168 (m), 1136 (m), 1041 (m), 877 (w), 795 (m), 753 (w), 690 (w), 656 (w), 583 (w), 521 (w), 510 (w), 447 (w) cm^{-1}. Anal. Calcd. (%) for $C_9H_9SnNO_4$: C, 34.44; H, 2.87; N, 4.46. Found: C, 35.01; H, 3.01; N, 4.73.

Spectroscopic data for 1-H_2O: IR (KBr): $\tilde{\nu}_{max}$: 3471 (br, w), 3132 (w), 2925 (w), 1697 (m), 1633 (s), 1484 (w), 1402 (m), 1327 (m), 1284 (w), 1162 (w), 1040 (w), 880 (w), 838 (m), 801 (m), 751 (w), 680 (w), 574 (w), 534 (w), 458 (w) cm^{-1}.

Tris[aqua-di-*n*-butyl-μ_2-(2,5-pyridinedicarboxylato-O,O′,N)tin] (2-H_2O). A solution of 2,5-pyridinedicarboxylic acid (0.25 g, 1.50 mmol) and di-*n*-butyltin(IV) oxide (0.37 g, 1.50 mmol) in toluene/ethanol (5:1) was refluxed for 8 h using a Dean−Stark trap. After cooling to room temperature, the solvent mixture was removed under vacuum, giving **2**-H_2O as a light yellow product that was washed with hot ethanol. Yield: 76%. mp 305−307 °C (dec). Crystals of $[\{(n\mathrm{Bu})_2\mathrm{Sn}(2,5\text{-pdc})(\mathrm{DMSO})\}_3\cdot 3\mathrm{DMSO}]$ (**2**-DMSO), $[\{[(n\mathrm{Bu})_2\mathrm{Sn}(2,5\text{-pdc})]\cdot 3\mathrm{MeOH}\cdot \mathrm{H_2O}\}_n]$ (**2**-MeOH), $[\{[(n\mathrm{Bu})_2\mathrm{Sn}(2,5\text{-pdc})(\mathrm{H_2O})]_3\cdot 1.5\mathrm{H_2O}\cdot 3\mathrm{EtOH}\}_n]$ (**2**-H_2O/EtOH), and $[\{[(n\mathrm{Bu})_2\mathrm{Sn}(2,5\text{-pdc})(\mathrm{H_2O})]_3\cdot 1.5\mathrm{H_2O}\cdot 3\mathrm{PrOH}\}_n]$ (**2**-H_2O/PrOH) were obtained after recrystallization of **2** from DMSO, MeOH, H_2O/EtOH,[13] and H_2O/PrOH, respectively.

Spectroscopic Data for 2-H_2O: IR (KBr): $\tilde{\nu}_{max}$: 3403 (br, w), 3052 (w), 2957 (m), 2926 (m), 2864 (m), 1642 (s), 1604 (s), 1486 (w), 1458 (w), 1404 (s), 1361 (m), 1284 (m), 1161 (w), 1089 (w), 1036 (w), 962 (w), 875 (w), 840 (m), 766 (w), 688 (w), 656 (s), 572 (w), 517 (w) cm^{-1}. MS (FAB$^+$): *m*/*z* (%): 1933.3 ($M_{pentanuc.}$−*n*Bu, 0.7), 1595.3 ($M_{tetranuc.}$, 1.7), 1533.2 ($M_{tetranuc.}$−Ph, 2), 1194.22 ($M_{trinuc.}$, 3.5), 1136.15 ($M_{trinuc.}$−*n*Bu, 7), 797.2 ($M_{dinuc.}$, 29), 400.1 ($M_{mononuc.}$, 100). Anal. Calcd. (%) for $C_{45}H_{63}Sn_3N_3O_{12}\cdot 3H_2O$: C, 43.30; H, 5.57; N, 3.37. Found: C, 43.82; H, 5.54; N, 3.61.

NMR Data in DMSO-*d*$_6$: ^{1}H NMR (400 MHz, DMSO-*d*$_6$, 20 °C, TMS) δ = 0.62 (t, 18H, CH_3), 1.08 (m, 12H, γ-CH_2), 1.31 (m, 24H, α-CH_2, β-CH_2), 8.38 (d, 3H, H3), 8.81 (dd, 3H, H4), 9.71 (dd, 3H, H5) ppm; ^{119}Sn NMR (149 MHz, DMSO-*d*$_6$, 20 °C, TMS) δ = −444 ppm. **NMR data in methanol-*d*$_4$:** ^{1}H NMR (400 MHz, MeOD, 20 °C, TMS) δ = 0.69 (t, 18H, CH_3), 1.17 (m, 24H, γ-CH_2), 1.53 (m, 12H, α-CH_2, β-CH_2), 8.53(d, 3H, H3), 9.01 (dd, 3H, H4), 9.83 (dd, 3H, H6) ppm; ^{119}Sn NMR (74.5 MHz, DMSO-*d*$_6$, 20 °C, TMS) δ = −412 ppm. **NMR data in pyridine-*d*$_5$:** ^{1}H NMR (400 MHz, pyridine-*d*$_5$, 20 °C, TMS) δ = 0.53 (t, 18H, CH_3), 1.04 (m, 12H, γ-CH_2), 1.44 (m, 12H, β-CH_2), 1.84 (m, 12H, α-CH_2), 8.87 (dd, 3H, H3), 9.16 (d, 3H, H4), 10.80 (s, 3H, H6) ppm; ^{13}C NMR (100 MHz, pyridine-*d*$_5$, 20 °C, TMS) δ = 13.8 (Cδ), 26.6 (Cγ), 28.8 (Cβ), 34.4 (Cα), 126.0 (C3), 133.6 (C5), 143.6 (C4), 149.3 (C6), 152.6 (C2), 166.2 (C7), 172.9 (C8) ppm; ^{119}Sn NMR (149 MHz, pyrdidine-*d*$_5$, 20 °C, TMS) δ = −426 (br) ppm.

Tris[aqua-diphenyl-μ_2-(2,5-pyridinedicarboxylato-*O*,*O*′,*N*)tin] (3-H_2O). A solution of 2,5-pyridinedicarboxylic acid (0.100 g, 0.598 mmol) and diphenyltin(IV) oxide (0.17 g, 0.598 mmol) in toluene/ethanol (5:1) was refluxed for 8 h using a Dean−Stark trap. After cooling to room temperature, the solvent mixture was removed under vacuum, giving **3**-H_2O as a light yellow product that was washed with hot ethanol. Yield: 81%. mp > 300 °C (dec). Crystals of $[\{(\mathrm{Ph_2Sn}(2,5\text{-pdc})(\mathrm{DMSO})\}_3\cdot 5\mathrm{DMSO}]$ (**3**-DMSO) were obtained after recrystallization of **3** from DMSO.

Spectroscopic Data for 3-H_2O: IR (KBr): $\tilde{\nu}_{max}$: 3430 (br, w), 3057 (w), 1645 (s), 1605 (s), 1486 (w), 1406 (s), 1364 (m), 1286 (w), 1158 (w), 1115 (w), 1039 (w), 992 (w), 877 (w), 844 (m), 766 (m), 733 (m), 693 (m), 578 (w), 520 (w), 457 (w) cm^{-1}. MS (FAB$^+$): *m*/*z* (%): 1314.02 ($M_{trinuc.}$), 1235.96 ($M_{trinuc.}$−Ph), 877.0 ($M_{dinuc.}$), 438.1 ($M_{mononuc.}$). Anal. Calcd. (%) for $C_{57}H_{39}Sn_3N_3O_{12}\cdot 3H_2O$: C, 50.04; H, 3.32; N, 3.07. Found: C, 49.40; H, 3.56; N, 3.26.

NMR Data in DMSO-*d*$_6$: ^{1}H NMR (400 MHz, DMSO-*d*$_6$, 20 °C, TMS) δ = 7.17 (m, 18H, *m*-C_6H_5, *p*-C_6H_5), 7.40 (m, 12H, *o*-C_6H_5), 8.45 (d, 3H, H3), 8.92 (dd, 3H, H4), 9.72 (s, br, 3H, H6) ppm; ^{13}C NMR (100 MHz, DMSO-*d*$_6$, 20 °C, TMS) δ = 125.3 (C3), 128.2 (*m*-C_6H_5), 128.4 (*p*-C_6H_5), 131.2 (C5), 133.1 (*o*-C_6H_5, $^2J_{Sn-C}$ = 70 Hz), 143.3 (C4), 147.3 (C6), 150.1 (*i*-C_6H_5), 150.8 (C2), 163.9 (C7), 171.7 (C8) ppm; ^{119}Sn NMR (149 MHz, DMSO-*d*$_6$, 20 °C, TMS) δ = −554 ppm.

X-ray Crystallography. X-ray diffraction studies were performed on a BRUKER-AXS APEX diffractometer with a CCD area detector ($\lambda_{MoK\alpha}$ = 0.71073 Å, monochromator: graphite). Frames were collected at T = 100 K (**2**-MeOH, **2**-H_2O/PrOH) and T = 293 K (**1**-H_2O, **2**-DMSO, **3**-DMSO) via ω− and Φ-rotation at 10 s per frame (SMART[20a]). The measured intensities were reduced to F^2 and corrected for absorption with SADABS (SAINT-NT[20b]). Structure solution, refinement, and data output were carried out with the SHELXTL-NT program package.[20c] The organic substituents of the R_2Sn moieties in the structures of **2**-DMSO, **2**-H_2O/PrOH, and **3**-DMSO are disordered so that restraints (DFIX and DANG) had to be introduced to obtain reasonable structural data. Furthermore, more or less disordered solvent molecules are present in the crystal lattices, which have been also restrained as far as necessary. In the case of **3**-DMSO, the disorder of the Sn-phenyl groups and especially of the five DMSO molecules present in the asymmetric unit are responsible for the somewhat high *R* values. Non-hydrogen atoms were refined anisotropically, while hydrogen atoms were placed in geometrically calculated positions using a riding model. The molecular and crystal structures were created by the BRUKER SHELXTL and MERCURY software packages.[20c,21] Crystallographic data for the structures reported in this article have been deposited with the Cambridge Crystallographic Data Centre as supplementary publications no. CCDC-242933−242937. Copies of the data can be obtained free of charge on application to CCDC, 12 Union Road, Cambridge CB2 1EZ, U.K. (fax: (+44)1223−336−033; e-mail: deposit@ccdc.cam.ac.uk; Web: www: http://www.ccdc.cam.ac.uk).

Acknowledgment. This work was supported by CONACyT. We thank Dr. Chip Cody from JEOL Company for his assistance in the realization of the mass spectra.

Supporting Information Available: Additional figures and tables giving the crystal data and structure refinement information, bond lengths and angles, atomic coordinates as well as isotropic and anisotropic displacement coordinates for all compounds that have been characterized by X-ray crystallography (PDF, CIF). This material is available free of charge via the Internet at http://pubs.acs.org.

JA0437095

---

(20) (a) *SMART: Bruker Molecular Analysis Research Tool*, version 5.618; Bruker AXS: Madison, WI, 2000. (b) *SAINT + NT*, version 6.04; Bruker AXS: Madison, WI, 2001. (c) *SHELXTL-NT*, version 6.10; Bruker AXS: Madison, WI, 2000.

(21) *Mercury*, version 1.1.2; Cambridge Crystallographic Data Centre: Cambridge, U.K., 2002.